water

MDPI

Article

Raw Rice Husk Biochar as a Potential Valuable Industrial Byproduct for the Removal of Rhodamine B from Water

Sedami Tozoun Romain Agassin [1], Jocinei Dognini [2] and Alexandre Tadeu Paulino [1,3,*]

[1] Post-Graduation Program in Applied Chemistry, Santa Catarina State University, Rua Paulo Malschitzki, 200, Zona Industrial Norte, Joinville 89219-710, SC, Brazil; romainagassin@gmail.com
[2] Instituto SENAI de Tecnologia Ambiental, Rua Harry Pofhal, 111, Escola Agrícola, Blumenau 89037-650, SC, Brazil; jocinei.dognini@sc.senai.br
[3] Department of Chemistry, Santa Catarina State University, Rua Paulo Malschitzki, 200, Zona Industrial Norte, Joinville 89219-710, SC, Brazil
* Correspondence: alexandre.paulino@udesc.br; Tel.: +55 (47) 3481-7926

Abstract: In this work, raw rice husk biochar (RRHB) was investigated for its potential as a valuable industrial byproduct for the decontamination of water using rhodamine B (RB) as a model pollutant. Specific functional chemical groups that were identified in the structure of the biochar using Fourier transform infrared (FTIR) spectra were determined to be responsible for the interaction between the biochar and the pollutant, explaining the sorption process. The interaction between the pollutant and biochar was also explained by the porosity of the sorbent, as demonstrated by scanning electron microscopy (SEM), and the specific surface area (Brunauer–Emmett–Teller analysis, BET). The ionic charge of the biochar structure was determined based on the point of zero charge (pH_{PCZ}). The best kinetic fit for the sorption of the dye on/in the biochar was obtained with the nonlinear pseudo-second-order and Elovich models. The nonlinear Freundlich isotherm had the best fit to the experimental data, and it was determined that the maximum sorption capacity was ~40 mg g^{-1}. The thermodynamic parameters indicated that the sorption of the RB on/in the RRHB was spontaneous. Overall, RRHB was demonstrated to be a potential biosorbent for cationic dyes such as RB. Finally, it is possible to recover the biosorbent, aggregating value to the byproduct and showing it to be an excellent option for use in water purification filters.

Keywords: sorption; biosorbent; pollution

Citation: Agassin, S.T.R.; Dognini, J.; Paulino, A.T. Raw Rice Husk Biochar as a Potential Valuable Industrial Byproduct for the Removal of Rhodamine B from Water. *Water* **2023**, *15*, 3849. https://doi.org/10.3390/w15213849

Academic Editor: Cidália Botelho

Received: 17 September 2023
Revised: 28 October 2023
Accepted: 2 November 2023
Published: 4 November 2023

1. Introduction

The preservation of water resources is indispensable, and as such, resources are necessary for studies on climate change as well as on the subsistence of the world population [1]. Both the causes and impacts of climate change are related to the use and reuse of water resources [2]. Thus, a joint set of actions involving governments, businesses, research institutes, universities, and society is essential to the preservation of these resources [3]. Access to water is indispensable for the eradication of hunger and poverty [4]. Approximately four billion people around the world face water scarcity at least one month per year [4–6]. To address this huge challenge, a set of measures should be taken to promote a sustainable policy for the monitoring, protection, and treatment of water resources [7]. Policies addressing the treatment of industrial, domestic, and hospital wastewater are essential in ensuring greater access to drinking water for the population and in minimizing the environmental impact of the improper disposal of wastewater [8,9].

In the current scenario of water scarcity throughout the world, there is a need for sustainable, economically feasible wastewater treatment technologies that are reproducible on an industrial scale and capable of the effective removal of different types of pollutants. Water treatment using byproducts from industrial production is an inexpensive, potentially feasible option that is easily applicable for the decontamination of waters containing

industrial dyes [10]. RRHB is a byproduct of the food industry that has been proposed for the sorption of pollutants with the possibility of decontaminating waters and aggregating value to the used sorbent material. Several sorbents have been tested for the removal of pollutants from water, including activated carbon, silica gel, activated alumina, zeolites, and synthetic resins [9–12]. Carbon-based materials such as RRHB are potential matrices for the sorption of hydrophilic pollutants due to their porous structures and large surface areas [13]. This facilitates intermolecular and intramolecular interactions between the pollutant and solid material [13]. As some carbon-based materials are hydrophobic, chemically inert, and show poor dispersion in water, they need to be modified to improve their sorption capacity and applicability in aqueous media [13]. However, the cost of the water treatment process when using activated and modified materials is higher compared to the cost of RRHB [14]. In this context, RRHB, without any modification, is a sorbent that could be a useful option for the removal of RB from water by controlling the sorption parameters.

RB (Figure 1) is a pollutant model that can be used in sorption studies during the development of water decontamination methods.

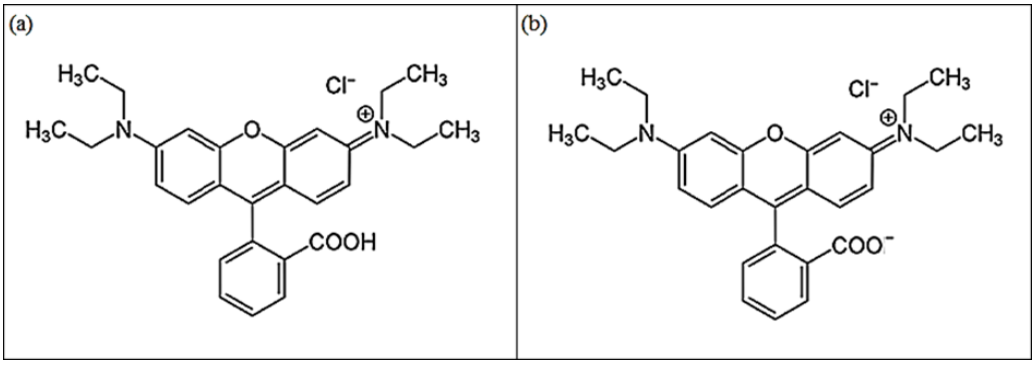

Figure 1. Molecular structure of RB in its cationic (**a**) and zwitterionic (**b**) forms.

It is a basic synthetic cationic dye classified as a xanthene due to its chromophore group [7]. This dye has a color index classified as basic violet 10, a molar mass of 479.02 g mol^{-1}, a wavelength between 547 and 555 nm for the absorption of electromagnetic radiation, a solubility in water of approximately 50.0 g L^{-1}, and a pKa value of 3.7 at 20.0 °C. RB can be used in acid and/or moderately acid baths due to the presence of a carboxyl group in its molecule and due to its zwitterionic structure [9,15]. The uses of RB include the dyeing of cotton, wool, silk, leather, paper, and bamboo. RB is also widely used as a biological stain in biomedical research labs due to its analytical and photochemical applications [16]. Although its zwitterionic form is neutral, it is generally considered to have a local charge due to the presence of ionizable groups [15]. RB is considered to be carcinogenic, genotoxic, and neurotoxic and causes harm to humans due to its interaction with cellular DNA, forming intermolecular hydrogen bonds that alter the physiological functions of cells [17,18]. However, RB is important for the monitoring of environmental pollution by pesticides because it is added to pesticide compositions to enhance the stability of these agricultural products [19].

Methods for the removal of organic pollutants such as RB from aqueous solutions include coagulation–flocculation [20], membrane filtration [21], electrocoagulation [22], electroflocculation [5,22], photodegradation [16,23], sorption [24], and so forth. From a practical and economic standpoint, sorption is important for the removal of diverse pollutants in water purification and refinement processes, as certain sorbents have intermolecular interactions with different solutes, enabling their effective separation from an aqueous medium [25]. For instance, RB can be removed from water by sorption on different activated carbon species, with a possibility of comparison with RRHB [26–28]. Moreover, different materials have demonstrated to be useful for the removal of other dyes such as

congo red, yellow 18, methylene blue, methyl violet, and nile blue from aqueous solutions via sorption [29,30].

Considering the possibility of aggregating value to rice husk by applying the biochar of this industrial byproduct in pollutant sorption studies, the aim of the present study was to demonstrate decontamination strategies for waters containing industrial dyes using RB as a model pollutant. For this, different experimental variables were studied, such as the sorption time, the pH of the solution, the temperature of the solution, and the stirring velocity. The interaction between the pollutant and biochar was determined based on the results of FTIR spectrometry. The morphology and specific surface area of the biochar were demonstrated using SEM and BET analyses, respectively. The pH_{PCZ} was determined to predict the ionic charge of the biochar structure. Sorption kinetics, isotherms, and thermodynamics were studied to enable the proposition of scaling methods for the decontamination of waters and the fabrication of a sorption filter. Overall, the innovation of the current work is related with the possibility of using RRHB as a sorbent, without any modification, for the removal of RB from aqueous solutions by controlling the sorption parameters and biochar properties. In addition to removing RB from solutions, it is possible to aggregate value to this industrial residue, which could be useful as a sorbent material in water purification filters in the textile industry.

2. Material and Methods

2.1. Reagents

All reagents were analytical grade and prepared using ultrapure water. RB was used with 100% purity. Sodium hydroxide (NaOH) with 100% purity, hydrochloric acid (HCl) with 35% purity, and analytical-grade ethanol were used as purchased. RRHB was acquired after the industrial processing of rice that was ground in a blender and converted into a powder, with the subsequent removal of silica by using alkaline hydrolysis.

2.2. Characterization of RRHB

FTIR spectrometric analyses were conducted in a Perkin-Elmer Frontier spectrometer with an attenuated total reflectance (ATR). The RRHB sample was previously prepared with potassium bromide (KBr) for the analyses using KBr pellets due to the chemical nature of the material. The range of the analysis was from 4000 to 500 cm^{-1}, with a resolution of 2.0 cm^{-1} and with 32 scans per sample. SEM images were recorded using a JSM-6701F scanning electron microscope with a magnification ranging from 200 to 5000 times, a distance of 12.3 mm, a tungsten cathode as the electron source, and an acceleration voltage of 15 kV. To determine the pH_{PCZ}, different solutions were prepared, and the initial pH (2.07, 3.64, 4.01, 5.07, 6.00, 7.28, 8.00, 9.48, 11.00, and 12.00) was adjusted using sodium hydroxide and hydrochloric acid (0.10 mol L^{-1}). The solutions were placed in contact with 0.10 g of the biochar for 24 h. The final pH of the solution was measured for the graphical determination of the pH_{PCZ}. This experiment was performed in triplicate with calculations of the respective standard deviation values. The BET method was employed to estimate the surface area and porosity of the material. This experiment was performed with a Quantachrome Nova 1000e analyzer operating between 77 and 273K with the sorption of ultrapure nitrogen gas onto the solid surface of the biochar. Each sample was previously treated at 250 °C for 12 h before the BET analysis. The pore distribution was estimated using the Barrett–Joyner–Halenda (BJH) method, and the specific surface area was estimated in the region of low pressure (p/p0) of 0.3028. the surface area was calculated using Equation (1):

$$S_{BET} = \frac{(m_m N_a A)}{MM} \quad (1)$$

in which m_m is the mass of molecules in a complete monolayer, N_a is the Avogadro constant, A is the surface area occupied by a nitrogen molecule, and MM is the molecular mass of nitrogen.

2.3. RB Sorption Tests

Standard RB solutions at different pH values (3.5, 4.0, 7.0, and 9.0), concentrations (1.0, 2.0, 3.0, 4.0, 5.0, and 6.0 mg L^{-1}), and temperatures (22.0, 45.0, 55.0, and 60.0 °C) were placed in 120 mL Erlenmeyer flasks containing different masses of RRHB (0.1, 0.5, 1.0, and 2.0 g). The mixtures were maintained for different sorption times (5, 15, 30, 45, 60, 90, 120, 150, 180, and 210 min) with different stirring velocities (2.0, 3.0, 4.0, and 5.0 rpm). The supernatant was removed from the solution and analyzed by measuring the absorbance using a UV-Vis spectrophotometer operating at 555 nm. All these experiments were performed in triplicate with calculations of the respective standard deviation values. The concentrations were estimated using an analytical calibration curve. The sorption capacity of the biochar was calculated using Equation (2):

$$q_t = \frac{(C_o - C_t)}{m} \cdot V \quad (2)$$

in which q_t is the sorption capacity of the biochar at a specific time t (mg g^{-1}), C_o and C_t are the initial concentration and concentration at a specific time t (mg L^{-1}), respectively, V (L) is the volume of the pollutant solution, and m (g) is the mass of the RRHB.

The removal efficiency (R, %) was calculated using Equation (3):

$$R,\ \% = \frac{(C_o - C_t)}{C_o} \cdot 100 \quad (3)$$

Pseudo-first-order [31], pseudo-second-order [32], Elovich [33], and intraparticle diffusion [34] kinetic models were used to estimate the sorption kinetics. Nonlinear Langmuir, Freundlich, Redlich–Peterson, and Sips isotherms [35,36] were used to predict the sorption mechanism, whereas the thermodynamics were studied considering the enthalpy, entropy, and free energy of the system [37,38].

2.4. RB Desorption Tests

Distilled water and ethanol were tested for the desorption of RB from the biochar, as the dye had a high solubility in both media. The desorption process was conducted using 0.10 g of biochar and 400 mL of solvent under stirring for 250 min. The desorption study was performed on two occasions (on the first and eighth days of sorption) to determine whether a change in the desorption would occur. The concentration of RB extracted from the biochar was measured using a UV-Vis spectrophotometer operating at 550 nm, and the recovery yield was calculated.

3. Results and Discussion

3.1. Characterization of RRHB

The FTIR spectra for the RRHB before and after the sorption process of RB, the SEM image at magnification of 5000 times, and the BET surface area related to the sorption of nitrogen gas on/in the biochar are presented in Figure 2.

The absorption band at 3434 cm^{-1} in the FTIR spectrum before the sorption of RB corresponded to hydroxyl groups (O-H) in the structure of the RRHB, which was also indicative of the presence of carbohydrate structures [39]. The composition of the natural fibers in the biochar may have alkanes, esters, aromatics, ketones, alcohols, and carboxylic acids that have oxygen and hydroxyl in the structure of their functional groups, which also assists in explaining the absorption bands between 1450 and 1600 cm^{-1}. The absorption band at 2918 cm^{-1} was due to symmetrical and asymmetrical vibrations of -CH_2- groups [40]. A band corresponding to the stretching of the C=O bond of conjugated ketones and aldehydes was found at 1635 cm^{-1} [41]. All the chemical groups identified in the structure of the RRHB are important to pollutant sorption studies and water decontamination processes. Similar absorption bands were found in the FTIR spectrum after the sorption of RB, with slight peak shifts and a decrease in the peak intensities due to intermolecular and intramolecular interactions among the cationic amino groups of the dye with the anionic

hydroxyl groups of the biochar. Moreover, hydrogen bonds between the dye and biochar enabled the occurrence of the sorption process, affecting the removal of the pollutants from the water [42].

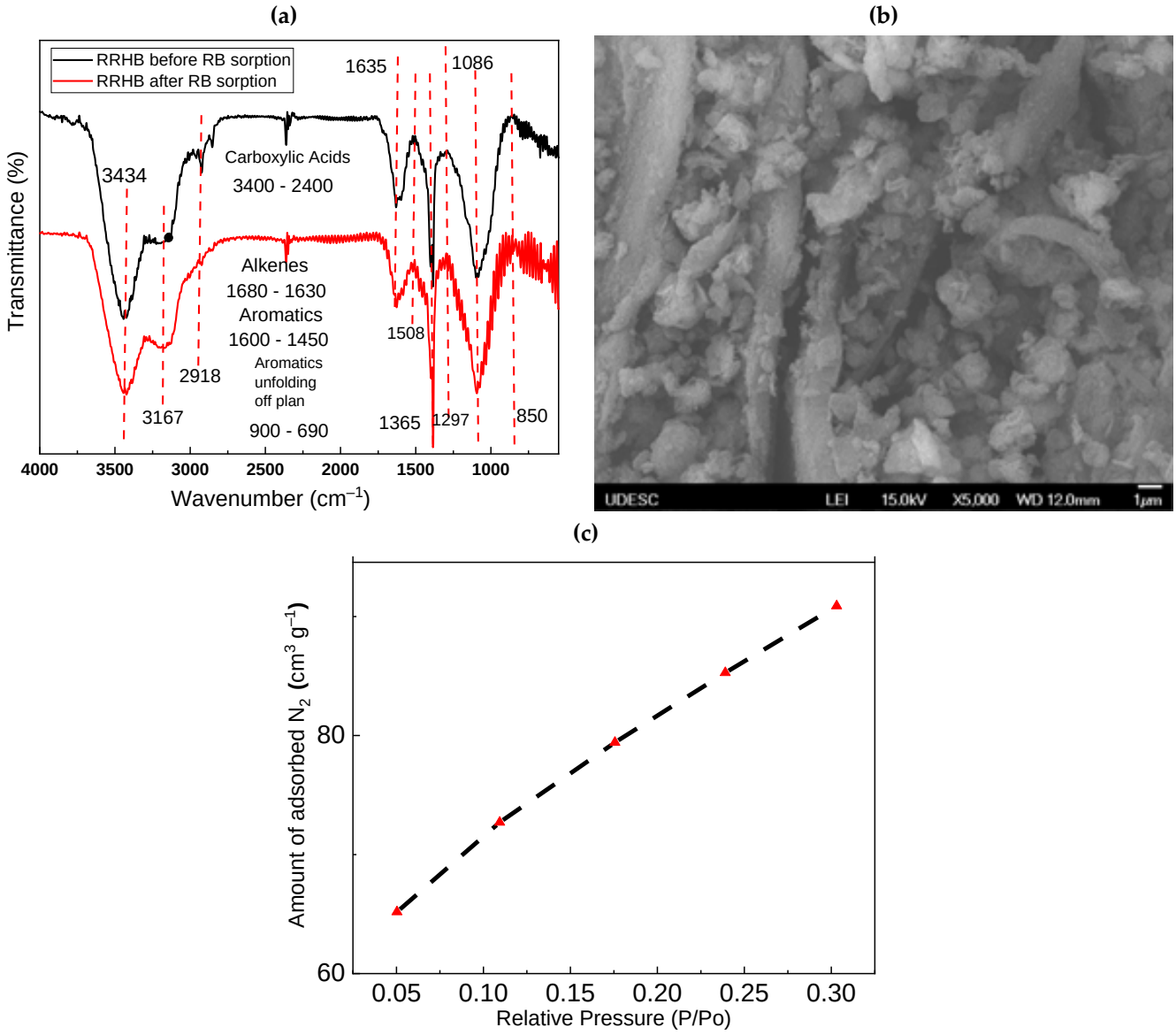

Figure 2. FTIR spectra for the RRHB before and after the sorption process of RB (**a**), SEM image at magnification of 5000 times (**b**), and BET surface area related to sorption of nitrogen gas on/in biochar (**c**).

The SEM image shows that the RRHB had a potentially irregular surface with various cavities. This morphology is interesting for sorption studies as it facilitates intermolecular and intramolecular interactions between the pollutant and solid material [32,42–44]. The morphological information is also important for the application of this material in pollutant sorption studies as it enables a better understanding of the sorption phenomena taking place on the surface and in the pores. By comparing the morphology of the biochar with the results of the BET analysis, the material structure could be better understood. High adsorption was seen at low N_2 pressures with the possibility of the formation of micropores. The surface area determined using the BET method was 267.9 m^2 g^{-1} with a total pore volume of 49.6 cm^3. Based on the distribution of the volume of pores as a function of the diameter, the biochar mainly had micropores with an average diameter of 224.0 Å.

Figure 3 displays the result for the pH_{PCZ} of the biochar, showing a value of 9.75.

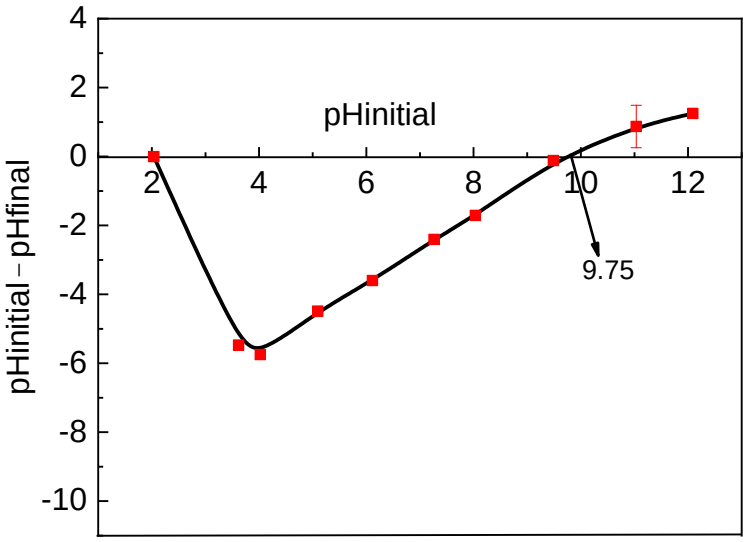

Figure 3. Point of zero charge (pH_{PCZ}) on surface of RRHB.

The sorption and electrostatic interactions of pollutants on/in solid structures can be explained by the pH_{PCZ} of the sorbent [45]. When the pH of a pollutant solution is less than the pH_{PCZ} of the sorbent (9.75 in the present case), the biochar surface tends to be positively charged, increasing the possibility of sorption studies of anionic species in solutions. In contrast, if the pH of the solution is higher than the pH_{PCZ}, the sorption of cationic species occurs on the biochar surface as the material tends to be negatively charged [46,47]. The results of the pH_{PCZ} analysis revealed a predominance of positive charges in the structure of the biochar between pH 2 and 4, a gradual increase in the quantity of negative charges with the increase in the pH between 4 and 9, and a predominance of negative charges at pH values higher than 9.75. Thus, the possibility of the sorption of cations and anions is expected between pH 4 and 9, depending on the pKa of the species of interest. By considering that RB is a zwitterionic species that has a pKa of 3.7, there will be predominance of negative charge on its structure at pH values higher than the pKa value, with the possibility of efficient sorption in the predominantly positive RRHB structure (pH below the pH_{PCZ} of the biochar) [48]. This effect is also minutely discussed in Section 3.2, confirming why higher sorption efficiencies of the RB were found at pH values ranging from 4 to 9. These surface data, together with the morphological and BET data, indicate that the RRHB investigated in this work is a potential option for studies on cationic and anionic species in aqueous solutions, depending on the pH of the medium and pKa of the species of interest.

3.2. RB Sorption Variables

Figure 4 presents the sorption capacity of the RB on/in the RRHB with variations in the sorption time and biochar mass.

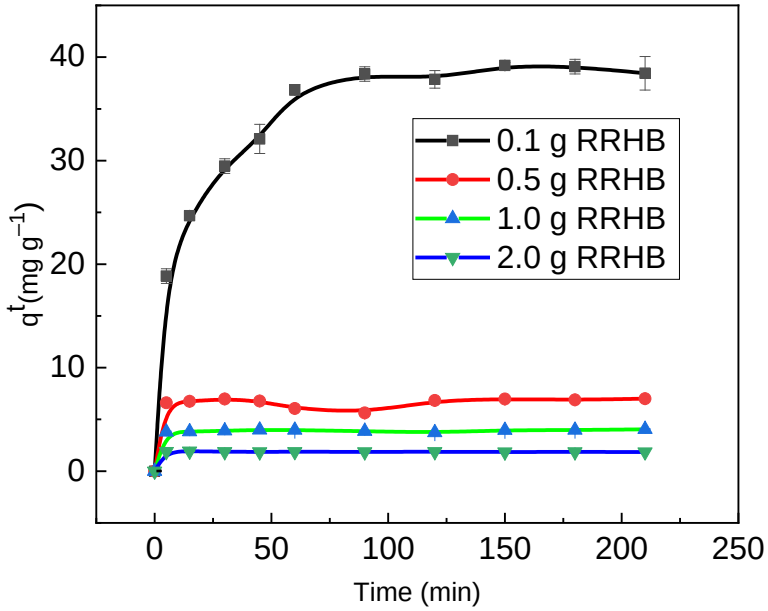

Figure 4. Sorption capacity of RB on/in RRHB with variations in sorption time and sorbent mass. Experimental conditions: initial concentration of RB = 4.0 mg L^{-1}; pH = 4.0; temperature = 22.0 °C; stirring = 3.0 rpm.

An increase in the sorption capacity was found with the increase in the biochar mass between 0.1 and 2.0 g. However, the greatest variation occurred with the use of 0.1 g of biochar mass, as a larger contact surface was available with a smaller mass for the interaction between the biochar and pollutant due to less aggregation of the material. Moreover, the concentration gradient at the solution/biochar surface interface was affected more by larger sorbent masses [49]. The largest change in the sorption capacity between masses of 0.5 and 2.0 g was around 2.0%, but this difference reached 97.7% between 0.1 and 2.0 g. As the sorbent mass is inversely proportional to the sorption capacity, an increase in the mass is expected to result in a reduction in the sorption capacity when the initial concentration is maintained and when the volume of the solution and the sorption time are constant. In such cases, intermolecular interactions between the sorbent and pollutant are disregarded. The sorption equilibrium using from 0.5 to 2.0 g of biochar occurred in 15 min due to the rapid saturation of the active sites available for interaction on the smaller available active surface area. In contrast, the sorption equilibrium occurred only between 180 and 210 min when 0.1 g was used.

Other variables of interest were the stirring velocity and the pH of the aqueous medium. The results of these analyses are shown in Figure 5a and Figure 5b, respectively.

No significant change in the sorption capacity (qt) was found with the increase in the stirring velocity from 2.0 to 5.0 rpm, with the exception of a velocity of 3 rpm. This may have occurred because slight desorption took place at certain velocities due to the effects of sorption kinetics [50]. Regarding the pH, the lowest quantity of dye removed beginning at 120 min was at pH 9.0, and the largest quantity was at pH 4.0 due to the pH_{PCZ} of the biochar and the pKa of the RB. The difference in the quantity of RB removed between pH 4.0 and 9.0 was due to the zwitterionic structure of the dye and the mixture of positive and negative charges in the structure of the biochar, as discussed in the pH_{PCZ} results. The lower sorption capacity at pH 3.5 is explained by the predominance of positive charges in the structure of both the biochar and the RB. At a very low pH, RB is expected to lose its zwitterionic structure, and a predominance of a cationic acid structure occurs in the solution [48], which hampers its sorption to positively charged surfaces such as that of the biochar. The greater RB sorption capacity at pH 4.0 may be explained by the predominance of negative charges in this zwitterion at pH values immediately above its pK_a and a predominance of positive charges in the structure of the biochar due to its

pH_{PCZ} [15]. This sorption capacity tends to diminish at pH values higher than 4.0 due to the tendency toward an increase in the anionic charge in the structure of the biochar with the deprotonation of functional groups containing hydroxyls, increasing the electrostatic repulsion forces between the sorbent and sorbate [51]. The reduction in the sorption capacity with the increase in the pH is also associated with the formation of hydrated RB ions and the increase in the size of the molecular structure, hampering intrapore diffusion and intermolecular interactions in the interior of the biochar structure [12]. Therefore, the more favorable pH value for the sorption of RB in the RRHB structure would be approximately 4.0, whereas the more unfavorable pH values would be those lower than 3.5 and approximately 9.0.

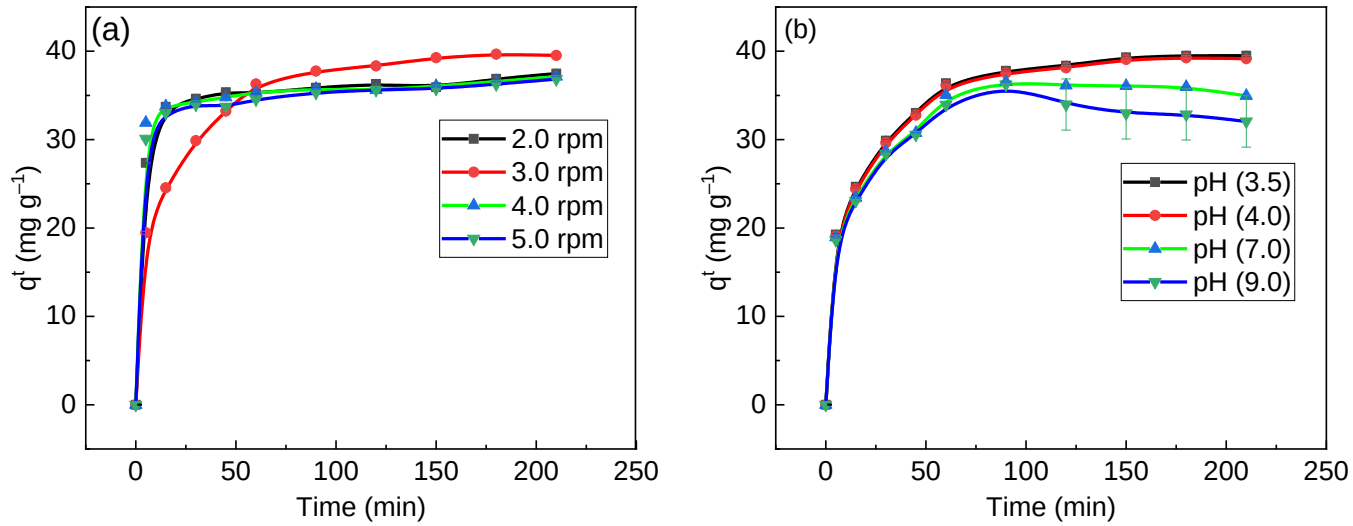

Figure 5. Effect of stirring of solution (**a**) with initial concentration of 4.0 mg L^{-1}, pH 4.0, temperature of 22.0 °C, and sorbent mass of 0.10 g. Effect of pH (**b**) with initial concentration of 4.0 mg L^{-1}, temperature of 22.0 °C, sorbent mass of 0.10, and stirring at 5.0 rpm.

3.3. RB Sorption Kinetics on/in Biochar

One of the objectives of sorption kinetics studies is to understand how resistance to mass transfer occurs between sorbents and sorbates [32]. The results of the nonlinear pseudo-first-order, pseudo-second-order, and Elovich kinetic models and the results of the intraparticle diffusion model are presented in Figure 6a–d, respectively, and in Table 1.

Table 1. Theoretical and experimental variables of kinetic models for sorption of RB on/in RRHB as industrial byproduct with aggregated value.

Kinetic Model	$Q_{maxcalc}$ (mg g^{-1})	$Q_{max\ ex}$ (mg g^{-1})	χ^2	k (min^{-1})	α	β	R^2	Adj.R^2
PFO	37.60	39.40	10.3	0.08			0.9303	0.9340
PSO	40.60	39.40	2.79	0.03			0.9810	0.9805
E			1.56		33.90	0.17	0.9902	0.9801
ID				2.28		0.78		0.7572

Note: Pseudo-first-order (PFO). Pseudo-second-order (PSO). Elovich (E). Intraparticle diffusion (ID). Unit of measure of k value for ID: mg g^{-1} $min^{-0.5}$.

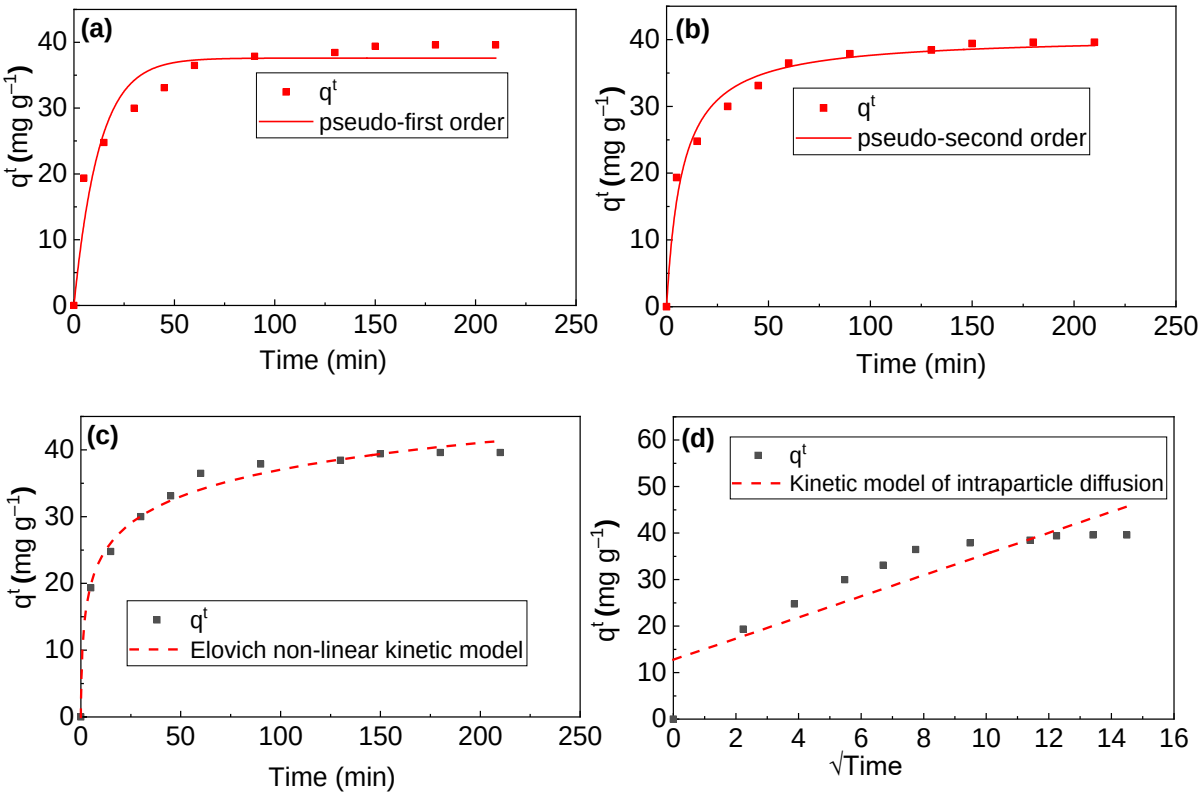

Figure 6. Nonlinear pseudo-first-order (**a**), pseudo-second-order (**b**), and Elovich (**c**) kinetics for sorption of RB on/in biochar. Intraparticle diffusion model (**d**). Experimental conditions: temperature = 22.0 °C; biochar mass = 0.1 g; pH = 4.0; initial concentration of RB = 4.0 mg L^{-1}; stirring = 3.0 rpm.

A much faster sorption of the pollutant occurred at the beginning of the experiment, which was followed by a significant reduction after 30 min due to the saturation of the active sites in the structure of the biochar [52]. The sorption equilibrium was reached after approximately 150 min of contact. The pseudo-second-order and Elovich kinetic models were the most suitable for explaining the sorption process based on the lower chi-square (χ^2) values and higher correlation coefficients (R^2 and Adj.R^2). The maximum experimental sorption capacity ($Q_{max\ exp}$) determined by the pseudo-second-order kinetic model was 39.4 mg of RB per g of biochar. This value was very similar to the calculated maximum sorption capacity ($Q_{max\ calc}$), which was 40.6 mg g^{-1}. The sorption coefficient (k) obtained by this kinetic model was 0.03 min^{-1}, indicating that the interaction at the biochar/RB interface occurred at a fast enough velocity to favor the process [32]. The intraparticle diffusion coefficient of 2.28 mg g^{-1} $min^{-0.5}$ suggests that this interaction occurred both on the surface and in the pores of the biochar during the RB sorption process. The initial sorption rate (α) determined by the Elovich kinetic model indicates a greater number of active sites available at the beginning of the sorption process, which explains the faster sorption in the first 30 min of the experiment. The low Elovich desorption constant (β) indicates that stronger intermolecular interactions took place during the sorption to the surface of the biochar. As the β value determined by the intraparticle diffusion model was a little larger, the forces of these interactions tended to diminish somewhat in the pores. In both cases, however, the RB interacted strongly enough with the biochar to be retained in its structure.

3.4. Sorption Isotherm of RB on/in Biochar

Table 2 presents the parameters of the nonlinear Langmuir, Freundlich, Sips, and Redlich–Peterson isotherms for the sorption of RB on/in the RRHB.

Table 2. Parameters of nonlinear Langmuir, Freundlich, Sips, and Redlich–Peterson isotherms for sorption of RB on/in RRHB. Experimental conditions: temperature = 22.0 °C; biochar mass = 0.1 g; pH = 4.0; initial concentration of RB = 4.0 mg L^{-1}; stirring = 3.0 rpm; sorption time = 250 min.

Model	Parameters
Langmuir	K_L = 3.67 × 10^{-4} L mg^{-1} R_L = 0.063 R^2 = 0.7709 χ^2 = 117.2
Freundlich	K_F = 1363.9 mg g^{-1} L mg^{-1} n_F = 3.34 R^2 = 0.9501 χ^2 = 21.0
Sips	K_s = 110.68 L mg^{-1} n_s = 1.0 × 10^{-10} R^2 = 0.77 χ^2 = 146.47
Redlich–Peterson	K_{RP} = 110.68 L mg^{-1} n_{RP} = 122.09 R^2 = 0.77 χ^2 = 146.47

The general profile found for the isotherms that best explained the experimental data was concave, indicating that the sorption process was favorable, which was in agreement with some thermodynamic data [53]. In this case, high quantities of RB were sorbed in small quantities of sorbates. Regardless of the predominance of physisorption in the surface interactions between the biochar and RB, chemical interactions could occur, especially in the pores [54]. The isotherm that best explained the experimental data of the RB sorption on/in the biochar was the nonlinear Freundlich model, which had a correlation coefficient (R^2) of 0.9501 and a chi-square (χ^2) value of 21.0. This implies that sorption occurred at multiple sites on both the surface and in the pores of the biochar, with interactions between the sorbed pollutant and neighboring active sorption sites. The Langmuir separation factor (R_L) was 0.063, suggesting that the RB interacted better with the solid phase (biochar) than the liquid phase (aqueous medium). Due to the very low pollutant concentration, the Langmuir model was not adequate for explaining the experimental results because this model assumes sorption on a homogenous surface, on which all sorption sites are identical and energetically equivalent. This diminishes the theoretical sorption capacity in comparison to the experimental sorption capacity [55]. With an n_F value of 3.34, the sorption process was assumed to be favorable [44]. However, this model is unable to predict or describe the sorption results at very high pollutant concentrations [37]. Moreover, the nonlinear Freundlich isotherm model is was to a linear model at low concentrations. There is experimental evidence of the distribution of energy among highly energetic active sorption sites with the formation of a strong bond between the sorbate and sorbent [56]. This explains the possibility of physical and chemical bonds during the sorption process of RB on/in biochar and the possibility of predicting the sorption process, as shown in Figure 7. The low n_s and high n_{RP} values are indications that the nonlinear Sips and Redlich–Peterson isotherm models were not useful for predicting the sorption mechanisms of the RB on/in the RRHB. This conclusion is also based on the low R^2 and high χ^2 values.

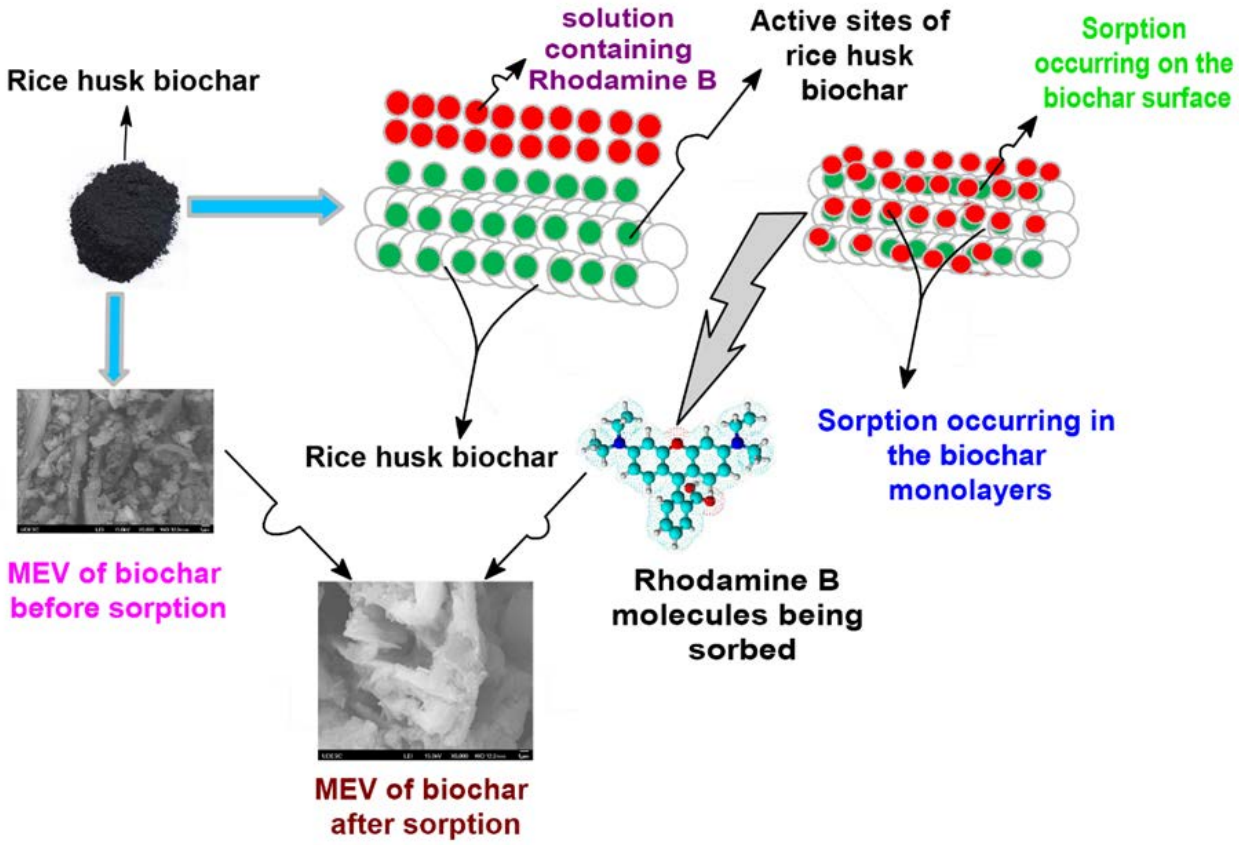

Figure 7. Schematic of sorption process of RB on/in RRHB.

3.5. Thermodynamics of Sorption of RB on/in Biochar

Figure 8 displays the thermodynamic results of the RB sorption on/in the biochar as a function of time and temperature. Table 3 displays the variations in the Gibbs free energy (ΔG°_{s}), sorption enthalpy (ΔH°_{s}), and sorption entropy (ΔS°_{s}).

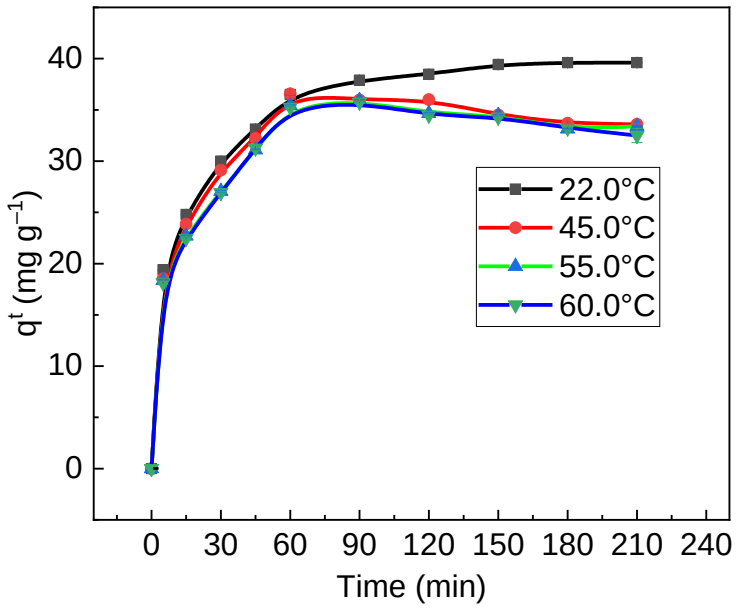

Figure 8. Results of thermodynamics for sorption of RB on/in biochar as function of time and temperature. Experimental conditions: initial concentration of RB = 4.0 mg L^{-1}; biochar mass = 0.1 g; pH = 4.0.

Table 3. Thermodynamic parameters for sorption of RB on/in RRHB.

Temperature (K)	Parameters			
	$\Delta G^{\circ}{}_{s}$ (J mol^{-1})	$\Delta H^{\circ}{}_{s}$ (J mol^{-1})	$\Delta S^{\circ}{}_{s}$ (J mol^{-1})	R^2
295.15	−6069.38	−6019.03	0.17	0.9802
318.15	−6073.31			
328.15	−6075.01			
333.15	−6075.87			

The reduction in temperature gradually increased the sorption capacity as a function of time until reaching equilibrium after 150 min. As the $\Delta G^{\circ}{}_{s}$ values were negative at all the temperatures studied, the sorption process was assumed to be spontaneous and favorable, which was compatible with the kinetic and isotherm results. The spontaneity of the reaction was practically invariable with the change in the temperature, indicating that $\Delta G^{\circ}{}_{s}$ was not a relevant thermodynamic parameter for explaining the change in the sorption of the RB on/in the biochar. The negative $\Delta H^{\circ}{}_{s}$ value indicates that the sorption process of the RB on/in the biochar was exothermic. In this case, the release of heat into the neighborhood during the exothermic process heats the medium and hampers the sorption of liquids to solid matrices [35], which explains the reduction in the sorption capacity of the RB on/in the RRHB by increasing the temperature values. Moreover, the $\Delta H^{\circ}{}_{s}$ value of –6019.03 J mol^{-1} was small enough to indicate surface physisorption during the process with the exchange of energy between the system and neighborhood. This type of surface interaction facilitates the recovery of sorbates in desorption processes. The positive $\Delta S^{\circ}{}_{s}$ value indicates that the interactions between the solute and solvent in the aqueous medium were stronger than the interactions between the RB and the biochar, with a consequent structural change occurring in both. Despite the positive $\Delta S^{\circ}{}_{s}$, the biochar had an excellent affinity for the RB and could be very useful for the purification of water and industrial effluents [57].

3.6. Recovery of RB and Biochar

The recovery of the RB from water was only 3.67% after eight days of contact, with a reduction in the recovery rate over time. This is only an indication of the removal of non-sorbed species or those with very weak intermolecular interactions on the surface of the biochar in this medium, despite the occurrence of the sorption process with physical and chemical interactions at multiple sites. The low desorption of the pollutant in this type of solvent is important for improving the efficiency of a water purification system. However, the average quantity of RB recovered after eight days of experimentation was 68.96% when ethanol was the eluent. In this case, greater interaction occurred between the RB and the solvent due to its greater solubility in ethanol [15]. This medium could be useful for the recovery of the pollutant and sorbent during the reutilization processes of an RB/RRHB system after some adjustments. Lastly, ethanol could be an option in a fixed-bed column to elute RB during column separation and purification processes.

4. Conclusions

The studies conducted in this work demonstrated the possibility of the sorption of RB on/in RRHB with the objective of proposing methods for the purification of water and wastewater from industries that process food and textile dyes. However, the control of some experimental variables in the medium (sorption time, pH, temperature, stirring velocity, and initial concentration of the pollutant) is required to achieve a high solute removal efficiency. Under the best experimental conditions, it was possible to remove up to 98% of the RB from the aqueous medium, which confirms the efficiency of the proposal. As the sorption process occurs with the formation of monolayers and a predominance of physisorption, the recovery and reuse of the biochar and pollutant is feasible, aggregating

value to this byproduct of industrial rice production. The maximum sorption capacity was around 40.0 mg of RB per g of biochar, with a recovery of approximately 70% using ethanol as the solvent. Thus, the sorption of cationic and anionic species on/in RRHB and the recovery of the biosorbent for reuse are possible. This aggregates value to an industrial byproduct that is currently discarded, avoiding environmental impacts and minimizing pollution from wastewater released from industries that use food and/or textile dyes in their systems.

Author Contributions: Data curation, formal analysis, investigation, roles/writing—original draft, S.T.R.A.; data curation, supervision, J.D.; conceptualization, funding acquisition, investigation, methodology, project administration, resources, writing—review and editing, A.T.P. All authors have read and agreed to the published version of the manuscript.

Funding: This research received no external funding.

Data Availability Statement: The datasets generated during and/or analyzed during the current study are available from the corresponding author on reasonable request.

Acknowledgments: ATP thanks FAPESC, Brazil for the financial support (grant number: 2023/TR331) and CNPq, Brazil for the research productivity fellowship (grant number: 313064/2022-9). This study was also funded in part by CAPES, Brazil—finance code 001.

Conflicts of Interest: The authors declare no conflict of interest.

References

1. Webb, J.; Hansen, W.; Desmond, A.; Fitzhugh, O. *Water and Climate Change*; Unesco: Paris, France, 2020.
2. Cabral, J.B.P.; Nogueira, P.F.; Becegato, V.A.; Becegato, V.R.; Paulino, A.T. Environmental Assessment and Toxic Metal-Contamination Level in Surface Sediment of a Water Reservoir in the Brazilian Cerrado. *Water* **2021**, *13*, 1044. [CrossRef]
3. Rosini, D.N.; Becegato, V.A.; Dalalibera, A.; Vilela, P.B.; Xavier, J.d.A.; Duminelli, E.C. Avaliação Da Qualidade Dos Sedimentos Em Áreas Agrícolas Do Município de Bom Retiro/SC. *Rev. Ibero-Am. Ciências Ambient.* **2020**, *11*, 79–93. [CrossRef]
4. FAO. Available online: https://www.fao.org/home/en/ (accessed on 17 September 2023).
5. Melchiors, M.S.; Piovesan, M.; Becegato, V.R.; Becegato, V.A.; Tambourgi, E.B.; Paulino, A.T. Treatment of Wastewater from the Dairy Industry Using Electroflocculation and Solid Whey Recovery. *J. Environ. Manag.* **2016**, *182*, 574–580. [CrossRef] [PubMed]
6. Pereira, A.G.B.; Rodrigues, F.H.A.; Paulino, A.T.; Martins, A.F.; Fajardo, A.R. Recent Advances on Composite Hydrogels Designed for the Remediation of Dye-Contaminated Water and Wastewater: A Review. *J. Clean. Prod.* **2021**, *284*, 124703. [CrossRef]
7. Ulusoy, H.İ. A Versatile Hydrogel Including Bentonite and Gallocyanine for Trace Rhodamine B Analysis. *Colloids Surf. A Physicochem. Eng. Asp.* **2017**, *513*, 110–116. [CrossRef]
8. Santhi, T.; Prasad, A.L.; Manonmani, S. A Comparative Study of Microwave and Chemically Treated Acacia Nilotica Leaf as an Eco Friendly Adsorbent for the Removal of Rhodamine B Dye from Aqueous Solution. *Arab. J. Chem.* **2014**, *7*, 494–503. [CrossRef]
9. Mchedlov-Petrosyan, N.O.; Kholin, Y.V. Aggregation of Rhodamine B in Water. *Russ. J. Appl. Chem.* **2004**, *77*, 414–422. [CrossRef]
10. Matias, C.A.; Guisolphi Gomes De Oliveira, L.J.; Geremias, R.; Stolberg, J. Biosorption of Rhodamine b from Aqueous Solution Using Araucaria Angustifolia Sterile Bracts. *Rev. Int. Contam. Ambient.* **2020**, *36*, 97–104. [CrossRef]
11. Tuzen, M.; Sarı, A.; Saleh, T.A. Response Surface Optimization, Kinetic and Thermodynamic Studies for Effective Removal of Rhodamine B by Magnetic AC/CeO2 Nanocomposite. *J. Environ. Manag.* **2018**, *206*, 170–177. [CrossRef]
12. da Silva Lacerda, V.; López-Sotelo, J.B.; Correa-Guimarães, A.; Hernández-Navarro, S.; Sánchez-Báscones, M.; Navas-Gracia, L.M.; Martín-Ramos, P.; Martín-Gil, J. Rhodamine B Removal with Activated Carbons Obtained from Lignocellulosic Waste. *J. Environ. Manag.* **2015**, *155*, 67–76. [CrossRef]
13. Jun, L.Y.; Mubarak, N.M.; Yee, M.J.; Yon, L.S.; Bing, C.H.; Khalid, M.; Abdullah, E.C. An Overview of Functionalised Carbon Nanomaterial for Organic Pollutant Removal. *J. Ind. Eng. Chem.* **2018**, *67*, 175–186. [CrossRef]
14. Liu, D.; Zhang, W.; Lin, H.; Li, Y.; Lu, H.; Wang, Y. A Green Technology for the Preparation of High Capacitance Rice Husk-Based Activated Carbon. *J. Clean. Prod.* **2016**, *112*, 1190–1198. [CrossRef]
15. Ramette, R.W.; Sandell, E.B. Rhodamine B Equilibria. *J. Am. Chem. Soc.* **1956**, *78*, 4872–4878. [CrossRef]
16. Yusuf, T.L.; Orimolade, B.O.; Masekela, D.; Mamba, B.; Mabuba, N. The Application of Photoelectrocatalysis in the Degradation of Rhodamine B in Aqueous Solutions: A Review. *RSC Adv.* **2022**, *12*, 26176–26191. [CrossRef]
17. Sulistina, D.R.; Martini, S. The Effect of Rhodamine B on the Cerebellum and Brainstem Tissue of *Rattus Norvegicus*. *J. Public Health Res.* **2020**, *9*, jphr.2020.1812. [CrossRef] [PubMed]
18. Sharma, J.; Sharma, S.; Bhatt, U.; Soni, V. Toxic Effects of Rhodamine B on Antioxidant System and Photosynthesis of Hydrilla Verticillata. *J. Hazard. Mater. Lett.* **2022**, *3*, 100069. [CrossRef]
19. Gao, W.; Wu, N.; Du, J.; Zhou, L.; Lian, Y.; Wang, L.; Liu, D. Occurrence of Rhodamine B Contamination in Capsicum Caused by Agricultural Materials during the Vegetation Process. *Food Chem.* **2016**, *205*, 106–111. [CrossRef]

20. Amalina, F.; Abd Razak, A.S.; Krishnan, S.; Zularisam, A.W.; Nasrullah, M. A Review of Eco-Sustainable Techniques for the Removal of Rhodamine B Dye Utilizing Biomass Residue Adsorbents. *Phys. Chem. Earth Parts A/B/C* **2022**, *128*, 103267. [CrossRef]
21. Tao, P.; Xu, Y.; Song, C.; Yin, Y.; Yang, Z.; Wen, S.; Wang, S.; Liu, H.; Li, S.; Li, C.; et al. A Novel Strategy for the Removal of Rhodamine B (RhB) Dye from Wastewater by Coal-Based Carbon Membranes Coupled with the Electric Field. *Sep. Purif. Technol.* **2017**, *179*, 175–183. [CrossRef]
22. Al-Gheethi, A.A.; Azhar, Q.M.; Senthil Kumar, P.; Yusuf, A.A.; Al-Buriahi, A.K.; Radin Mohamed, R.M.S.; Al-shaibani, M.M. Sustainable Approaches for Removing Rhodamine B Dye Using Agricultural Waste Adsorbents: A Review. *Chemosphere* **2022**, *287*, 132080. [CrossRef]
23. Paz, M.J.; Vieira, T.; Enzweiler, H.; Paulino, A.T. Chitosan/Wood Sawdust/Magnetite Composite Membranes for the Photodegradation of Agrochemicals in Water. *J. Environ. Chem. Eng.* **2022**, *10*, 106967. [CrossRef]
24. Abdolrahimi, N.; Tadjarodi, A. Adsorption of Rhodamine-B from Aqueous Solution by Activated Carbon from Almond Shell. In Proceedings of the 23rd International Electronic Conference on Synthetic Organic Chemistry, Online, 15 November–15 December 2019; p. 51.
25. Vieira, T.; Artifon, S.E.S.; Cesco, C.T.; Vilela, P.B.; Becegato, V.A.; Paulino, A.T. Chitosan-Based Hydrogels for the Sorption of Metals and Dyes in Water: Isothermal, Kinetic, and Thermodynamic Evaluations. *Colloid Polym. Sci.* **2021**, *299*, 649–662. [CrossRef]
26. Alhogbi, B.G.; Altayeb, S.; Bahaidarah, E.A.; Zawrah, M.F. Removal of Anionic and Cationic Dyes from Wastewater Using Activated Carbon from Palm Tree Fiber Waste. *Processes* **2021**, *9*, 416. [CrossRef]
27. Yahya, M.A.; Al-Qodah, Z.; Ngah, C.W.Z. Agricultural Bio-Waste Materials as Potential Sustainable Precursors Used for Activated Carbon Production: A Review. *Renew. Sustain. Energy Rev.* **2015**, *46*, 218–235. [CrossRef]
28. Bonyadi, Z.; Kumar, P.S.; Foroutan, R.; Kafaei, R.; Arfaeinia, H.; Farjadfard, S.; Ramavandi, B. Ultrasonic-Assisted Synthesis of Populus Alba Activated Carbon for Water Defluorination: Application for Real Wastewater. *Korean J. Chem. Eng.* **2019**, *36*, 1595–1603. [CrossRef]
29. Angin, D. Utilization of Activated Carbon Produced from Fruit Juice Industry Solid Waste for the Adsorption of Yellow 18 from Aqueous Solutions. *Bioresour. Technol.* **2014**, *168*, 259–266. [CrossRef]
30. Foroutan, R.; Mohammadi, R.; Ramavandi, B. Elimination Performance of Methylene Blue, Methyl Violet, and Nile Blue from Aqueous Media Using AC/$CoFe_2O_4$ as a Recyclable Magnetic Composite. *Environ. Sci. Pollut. Res.* **2019**, *26*, 19523–19539. [CrossRef]
31. Lagergren, S. About the Theory of So-Lagergren, S. About the Theory of so-Called Adsorption of Solid Substance. *Handlinger* **1898**, *24*, 1–39. [CrossRef]
32. Ho, Y.S.; Ng, J.C.Y.; McKay, G. Kinetics of Pollutant Sorption by Biosorbents: Review. *Sep. Purif. Methods* **2000**, *29*, 189–232. [CrossRef]
33. Wu, F.-C.; Tseng, R.-L.; Juang, R.-S. Characteristics of Elovich Equation Used for the Analysis of Adsorption Kinetics in Dye-Chitosan Systems. *Chem. Eng. J.* **2009**, *150*, 366–373. [CrossRef]
34. Russo, V.; Rossano, C.; Salucci, E.; Tesser, R.; Salmi, T.; Di Serio, M. Intraparticle Diffusion Model to Determine the Intrinsic Kinetics of Ethyl Levulinate Synthesis Promoted by Amberlyst-15. *Chem. Eng. Sci.* **2020**, *228*, 115974. [CrossRef]
35. Wang, J.; Guo, X. Adsorption Isotherm Models: Classification, Physical Meaning, Application and Solving Method. *Chemosphere* **2020**, *258*, 127279. [CrossRef]
36. Al-Ghouti, M.A.; Da'ana, D.A. Guidelines for the Use and Interpretation of Adsorption Isotherm Models: A Review. *J. Hazard. Mater.* **2020**, *393*, 122383. [CrossRef] [PubMed]
37. Vieira, T.; Becegato, V.A.; Paulino, A.T. Equilibrium Isotherms, Kinetics, and Thermodynamics of the Adsorption of 2,4-Dichlorophenoxyacetic Acid to Chitosan-Based Hydrogels. *Water Air Soil Pollut.* **2021**, *232*, 60. [CrossRef]
38. Filho, W.B.F.; Agassin, S.T.R.; Naidek, K.P.; Paulino, A.T. Pectin Hydrogels Modified with Montmorillonite: Case Studies for the Removal of Dyes and Herbicides from Water. *J. Environ. Chem. Eng.* **2023**, *11*, 110846. [CrossRef]
39. Pereira, A.G.B.; Martins, A.F.; Paulino, A.T.; Fajardo, A.R.; Guilherme, M.R.; Faria, M.G.I.; Linde, G.A.; Rubira, A.F.; Muniz, E.C. Recent Advances in Designing Hydrogels from Chitin and Chitin-Derivatives and Their Impact on Environment and Agriculture: A Review. *Rev. Virtual Quim.* **2017**, *9*, 370–386. [CrossRef]
40. Hanauer, D.C.; de Souza, A.G.; Cargnin, M.A.; Gasparin, B.C.; Rosa, D.d.S.; Paulino, A.T. Pectin-Based Biohydrogels Reinforced with Eucalyptus Sawdust: Synthesis, Characterization, β-D-Galactosidase Immobilization and Activity. *J. Ind. Eng. Chem.* **2021**, *97*, 368–382. [CrossRef]
41. Asadullah, M.; Asaduzzaman, M.; Kabir, M.S.; Mostofa, M.G.; Miyazawa, T. Chemical and Structural Evaluation of Activated Carbon Prepared from Jute Sticks for Brilliant Green Dye Removal from Aqueous Solution. *J. Hazard. Mater.* **2010**, *174*, 437–443. [CrossRef]
42. Lopez-Sanchez, P.; Martinez-Sanz, M.; Bonilla, M.R.; Wang, D.; Gilbert, E.P.; Stokes, J.R.; Gidley, M.J. Cellulose-Pectin Composite Hydrogels: Intermolecular Interactions and Material Properties Depend on Order of Assembly. *Carbohydr. Polym.* **2017**, *162*, 71–81. [CrossRef]
43. Tolls, J. Sorption of Veterinary Pharmaceuticals in Soils: A Review. *Environ. Sci. Technol.* **2001**, *35*, 3397–3406. [CrossRef]
44. Delle Site, A. Factors Affecting Sorption of Organic Compounds in Natural Sorbent/Water Systems and Sorption Coefficients for Selected Pollutants. A Review. *J. Phys. Chem. Ref. Data* **2001**, *30*, 187–439. [CrossRef]

45. Bakatula, E.N.; Richard, D.; Neculita, C.M.; Zagury, G.J. Determination of Point of Zero Charge of Natural Organic Materials. *Environ. Sci. Pollut. Res.* **2018**, *25*, 7823–7833. [CrossRef]
46. Matias, C.A.; Vilela, P.B.; Becegato, V.A.; Paulino, A.T. Adsorption and Removal of Methylene Blue from Aqueous Solution Using Sterile Bract of Araucaria Angustifolia as Novel Natural Adsorbent. *Int. J. Environ. Res.* **2019**, *13*, 991–1003. [CrossRef]
47. Aparecida Matias, C.; Vilela, P.B.; Becegato, V.A.; Paulino, A.T. Adsorption Kinetic, Isotherm and Thermodynamic of 2,4-Dichlorophenoxyacetic Acid Herbicide in Novel Alternative Natural Adsorbents. *Water Air Soil Pollut.* **2019**, *230*, 276. [CrossRef]
48. Goto, Y.; Nema, Y.; Matsuoka, K. Removal of Zwitterionic Rhodamine B Using Foam Separation. *J. Oleo Sci.* **2020**, *69*, 563–567. [CrossRef] [PubMed]
49. Núñez-Delgado, A.; Álvarez-Rodríguez, E.; Fernández-Sanjurjo, M.J.; Fernández-Calviño, D.; Conde-Cid, M.; Arias-Estévez, M. Introduction. In *Sorbents Materials for Controlling Environmental Pollution*; Elsevier: Amsterdam, The Netherlands, 2021; pp. 1–12.
50. Soares, J.d.P.; Souza, J.A.d.; Cavalheiro, É.T.G. Characterization of Commercial Samples of Vermicompost from Bovine Manure and Evaluation of the Influence of PH and Time on Co(II), Zn(II) and Cu(II) Adsorption. *Quim. Nova* **2004**, *27*, 5–9. [CrossRef]
51. Ahmad, R.; Kumar, R. Adsorption Studies of Hazardous Malachite Green onto Treated Ginger Waste. *J. Environ. Manag.* **2010**, *91*, 1032–1038. [CrossRef] [PubMed]
52. Machado, A.A.; Da Rosa, A.L.D.; Carissimi, E. Adsorption of Rhodamine B onto Commercial Activated Coal. *Rev. CIATEC-UPF* **2019**, *11*, 100–107. [CrossRef]
53. McCabe, W.; Smith, J.; Harriott, P. *Unit Operations of Chemical Engineering*, 7th ed.; McGraw-Hill Education: New York, NY, USA, 2005.
54. Giles, C.H.; MacEwan, T.H.; Nakhwa, S.N.; Smith, D. Studies in Adsorption. Part XI. A System of Classification of Solution Adsorption Isotherms, and Its Use in Diagnosis of Adsorption Mechanisms and in Measurement of Specific Surface Areas of Solids. *J. Chem. Soc.* **1960**, *111*, 3973–3993. [CrossRef]
55. Bansal, R.C.; Goyal, M. *Activated Carbon Adsorption*; CRC Press: Boca Raton, FL, USA, 2005; ISBN 9781420028812.
56. Cooney, D.O. *Adsorption Design for Wastewater Treatment*; CRC Press: Boca Raton, FL, USA, 1998.
57. Do Nascimento, R.F.; de Lima, A.C.A.; Vidal, C.B.; Melo, D.d.Q.; Raulino, G.S.C. *Adsorção: Aspectos Teóricos e Aplicações Ambientais*, 1st ed.; UFC, Editora: Fortaleza, Bazil, 2014; ISBN 9788574851860.